FINAL PROGRESS REPORT

TO

THE NATIONAL AERONAUTICS AND SPACE ADMINISTRATION

FOR GRANT NO. NAG 5-879

"A Program to Study Antiprotons in the Cosmic Rays — Arizona Collaboration"

Theodore Bowen, Principal Investigator

Department of Physics

University of Arizona

Tucson, AZ 85721

THE LEAP CHERENKOV DETECTOR EMPLOYING FLUOROCARBON LIQUID IN A MAGNETIC FIELD

T. BOWEN[1] and A. MOATS[2]

[1] *Department of Physics, University of Arizona, Tucson, AZ 95721, USA*

[2] *Sandia National Laboratories, Div. 1272, P.O. Box 5800, Albuquerque, NM 87185, USA*

The Cherenkov detector designed and built for the LEAP (Low Energy AntiProton) experiment utilized a novel design to achieve appreciable sensitive area (0.2 m^2) with a refractive index of 1.25 in a magnetic fringe field region (500-1000 Gauss). The weight was held to only 64 kg by using 16 unshielded Hamamatsu R2490-01 photomultiplier tubes, each aligned with its local magnetic field. A filling and reservoir system for the highly volatile FC-72 liquid Cherenkov radiator also presented many design challenges. Relativistic particles yielded about 72 photoelectrons, total.

1. Introduction

On August 21, 1987, the LEAP (Low-Energy AntiProton) experiment was launched from Prince Albert, Canada, for a 20-hour flight at a residual atmospheric thickness of 4.7 g/cm^2. LEAP, a high-altitude balloon-borne antiproton search, is a collaboration of groups at NASA/Goddard Space Flight Center, New Mexico State University, and the University of Arizona. The principal components of LEAP are the NMSU magnet spectrometer, GSFC time-of-flight (TOF) counters, and a UA Cherenkov counter. A schematic of the experimental stack is shown in fig. 1. The magnet spectrometer, described in detail elsewhere [1], measures the charge sign and rigidity of particles by tracing their trajectories using eight planes of x-y multiwire proportional counters (MWPCs) in a magnetic field produced by a superconducting magnet coil. For a $Z = 1$ particle, the magnetic rigidity is numerically equal to the particle momentum. The TOF system, described in reference [2], consists of four planes (two above the magnet, two below the magnet) of plastic scintillator slabs that were viewed by photomultiplier tubes at one end of each slab. The TOF system

measured the velocity of the incoming particles and was sufficiently accurate for particle identification below 500 MeV.

The Cherenkov counter, described here, was designed and built by the Arizona group to extend the energy range of LEAP to 1.2 GeV, as well as identify spurious background events due to electrons, muons, or pions. Protons and antiprotons with less than 1.2 GeV kinetic energy radiate less than 1/2 of the maximum Cherenkov light intensity; in the same rigidity range lighter particles, such as electrons, muons, and pions, radiate nearly the maximum intensity. The Cherenkov counter could then effectively separate the heavier protons from the relatively light background particles. Thus, the counter was indispensable to the identification of antiprotons above 600 MeV kinetic energy, since the TOF system was not sufficiently accurate at those energies to separate antiprotons from the lighter cosmic ray cascade background particles. In addition, the Cherenkov counter served as a veto against electrons, muons, and pions for the analysis of the lower energy data. Because of the high magnetic field region in which the detector was positioned and additional weight and size constraints, the Cherenkov counter utilized a novel design. The total weight for this counter was 64 kg.

Directly below the Cherenkov counter was a plastic scintillation counter (S2), that recorded the exit of particles from the bottom of the Cherenkov counter. At the top of the LEAP stack, a scintillation detector (S1) was used to determine the magnitude of the particles' charge and, in combination with S2, was an additional rough check on the TOF and travel direction. Thus, the LEAP experiment was designed to detect antiprotons in the 120 MeV to 1.2 GeV kinetic energy range.

2. The counter

In essence, the Cherenkov counter consists of a box filled with FC72, a liquid fluorocarbon which emits Cherenkov radiation whenever charged particles pass through the

liquid with a velocity exceeding the speed of light in this medium. Assuming a constant index of refraction (n), the Cherenkov light intensity ratio [3],

$$\frac{I_c}{I_{c,max}} = \frac{1 - 1/(n\beta)^2}{1 - 1/(n)^2} \ , \tag{1}$$

where I_c is the Cherenkov light intensity and $I_{c,max}$ is the maximum light emitted for a $Z = 1$ highly relativistic particle, is a function only of velocity β and n. In fig. 2, $I_c/I_{c,max}$ is plotted as a function of the particle kinetic energy for several values of n. To separate the heavier protons and antiprotons form electrons, muons, and pions, we required the protons in the rigidity range of interest to radiate less than about 50% of $I_{c,max}$, while the pions in the same rigidity range radiate close to $I_{c,max}$. For intensities $\leq (1/2)I_c/I_{c,max}$ the proton/antiproton curve in fig. 2 has a steep slope and is thus in the most sensitive range for gathering information on velocity. While any index of refraction between 1.10 and 1.33 would distinguish antiprotons from electrons, muons, and pions, the refractive index must be about 1.25 in order to identify antiprotons in an energy range which extends the LEAP energy range above that of the accurate energy range of the TOF system.

Liquid fluorocarbon FC72 [4] was found to be an appropriate medium because of its 1.25 index of refraction, its low coefficient of absorption in the visible and ultraviolet, and the slow variation of n as a function of wavelength. The results of our optical measurements of n are presented in fig. 3. Among the fluorocarbon fluids, FC72 was the least expensive and, at 1.68 g/cm^2, the least dense.

2.1. Enclosures for liquid and light

In the final design, the liquid FC72 was held in an acrylic box with inside dimensions of 438 mm × 438 mm × 121 mm. This box was viewed by 16 Hamamatsu R2490-01 photomultiplier tubes (PMTs) held in place by an aluminum box that surrounded the acrylic box (see fig. 4). The acrylic box was constructed of UVA (ultraviolet absorbing) material, with 9.5 mm thick side walls and 4.8 mm thick top and bottom walls. As shown in fig. 4, the box had two projections, a filling nipple and a venting nipple, allowing hoses

to be attached for the filling and emptying of FC72 into and out of the box. The inside surface was coated with a waveshifter mixture (p-Terphenyl, Bis-MSB, and PPO) referred to as "blue waveshifter" by Viehmann and Frost [5]. The waveshifter allowed us to detect UV photons in addition to those in the visible. Since the coating was on the inner surface of the box, UVT (ultraviolet transmitting) acrylic was not necessary. In fact, we specifically avoided UVT acrylic, since, in the past, it had been found to emit scintillation light [6].

The acrylic box surrounding the FC72 liquid radiators avoids the problems of windows and seals at each PMT or placing the PMTs inside the liquid, but a small penalty is paid - the top and bottom acrylic walls of the box contribute to the Cherenkov light. At the threshold for $n = 1.25$, the box contributes a background equivalent to 6% of the maximum light output of the liquid radiator. At 1.2 GeV proton kinetic energy, this becomes 10%. Below the threshold for $n = 1.25$, the background light persists down to a Cherenkov threshold at proton kinetic energy $E = 320$ MeV.

Immediately surrounding the transparent acrylic box was an aluminum box, providing the necessary light-tightness and mechanical support for the PMTs. The bottom and sides, excluding the PMT holders (the projections on the four sides), was cut from a single piece of 1.6 mm thick aluminum and folded into position. The seams and cylindrical PMT holders were welded together. The top is a separate removable piece, complete with projections that allow clearance for the acrylic fill and vent nipples, and for their attached tubing to be fed through to the outside. The top piece was attached to the rest of the box with black optical tape. Outside the aluminum box the top and bottom walls were supported by 13 mm thick sheets of aluminum Hexcel, and the fluid inside was maintained at a slight positive pressure relative to the outside. The inside surface of the aluminum box was painted with Eastman Kodak $BaSO_4$ paint. This highly reflective paint [7] allowed us to collect a large fraction of the Cherenkov light generated by each particle. Sixteen 51 mm diameter Hamamatsu PMTs viewed this box, each PMT face bordered by a 6 mm radial width non-reflective area (the layers of 6 mm thick foam plastic used to stabilize the

tubes in position). The calculated efficiency factor of the white box was 0.33, assuming a reflectivity of 0.992 for the white paint.

2.2. Photomultiplier tubes

The Hamamatsu R2490-01 PMTs were selected because of their ability to operate without magnetic shielding in the 500-1000 Gauss magnetic spectrometer fringe field present at the counter's position, provided that each PMTs axis is parallel within 5° to the local magnetic field direction. If heavy iron shields had been necessary, they would have distorted the spectrometer field, requiring intensive mapping of the field as well as adding significantly to the total weight of the experiment. To accommodate the Hamamatsu tubes, each projection of the aluminum box had to be attached at a specific angle, which was calculated utilizing a computer model of the LEAP magnetic field. The numerical solution for the field was obtained by modeling the magnet coil (seen as a thick band of current) as an array of infinitesimally thin circular loops of current [8].

2.3. Filling system

The filling system designed to fill the counter with FC72 while in place in the LEAP system is shown in fig. 5. A careful design was necessary to satisfy the following requirements: The filling system must, first of all, be able to completely fill the counter, without bubbles, and drain the counter completely while in place in the LEAP gondola without being able to visually inspect inside the counter. The system must be able to accommodate any pressure changes in the gondola (equalizing the pressure between the FC72 and the gondola atmosphere) and any volume changes in the FC72 liquid (due to temperature changes). The filling system must preserve the light-tightness of the Cherenkov counter. Finally, the system must not spill, leak, or evaporate the volatile FC72 fluid, even when the gondola tips over on landing to avoid contamination of the other LEAP detectors and loss of the FC72 (the counter contained about $1000 US worth of FC72).

Two lines of clear polyethylene tubing, 6.4 mm inner diameter, attached to the inlet and vent nipples of the acrylic box, were fed through the aluminum box, and were

then attached to sections of copper tubing, each formed into four helical turns. The clear tubing between the aluminum box and the copper helices was covered with two layers of black shrink-wrap electronic spaghetti tubing. The shrink-wrap and the copper tubing spirals prevented light from entering the counter through the inlet and outlet tubing, completing the light-tightness of the system. Both the fill and vent lines were attached to an outside translucent polyethylene reservoir [9] directly exposed to atmospheric pressure with a capacity of two liters. This reservoir allows the FC72 to thermally expand and contract during the flight without excessively pressurizing and damaging the acrylic box, while maintaining a liquid pressure about 200 mm above the outside pressure. To discourage evaporation of the fluid, the reservoir lid was vented via a long 3.2 mm diameter tube that circled the inner wall of the gondola for two full turns. This circular vent tube provided a long diffusion length of approximately 10 m, yet would prevent fluid leakage if the gondola did not land upright after the flight.

The lines and valves shown in fig. 5 allowed us to fill the counter without air bubbles in the counter itself or in any of the filling system lines. While filling, the counter was tilted slightly so that the vent outlet was at the counter's highest point, forcing air bubbles in the counter up the vent line. At the end of a filling cycle, the FC72 fluid level was visible through the translucent walls of the fluid reservoir, ensuring that the counter was completely filled. A complete set of written instructions for filling and draining procedures, developed before final assembly with the acrylic box clamped between wood supports, helped to prevent costly errors.

2.4. High voltage adjustments

The PMTs were divided into two groups of eight, with each group connected to a Spellman 3 KV high voltage supply through series voltage-adjusting potentiometers for each PMT. The high voltage adjustments were balanced during final assembly for equal PMT outputs using a light source that we constructed. The light source used the conversion electrons (662 keV) from a point Cs^{137} source embedded in a 2.5 mm radius sphere of plastic

scintillator to provide a fixed pulse of light. At this thickness, the conversion electrons would deposit essentially all of their ionization energy loss in the surrounding scintillator, but the gamma-ray background due to Compton recoil electrons was minimized. The resulting pulse height distributions from each Hamamatsu PMT were measured with a LeCroy model 3001 multi-channel analyzer in the charge-integrating mode. Each PMT was set at a point that corresponded to a gain of approximately 10^6.

2.5. Output electronics

The LEAP stack used both NIM and CAMAC electronics. A logic diagram for the LEAP experiment as a whole is shown elsewhere [11]. Pulses from the Cherenkov PMTs were amplified a factor of 10 separately for each PMT using Avantek GPD-110 100 MHz high frequency amplifiers before entering LeCroy 2249 ADCs. The signal from S2 was also analyzed by one of these ADCs and, in addition, a signal splitter allowed us to use a TDC for a rough TOF from the S1-S2 signals. An event would trigger the LEAP stack whenever there was at least one "hit" in each of the four TOF planes. The readout was also programmed such that a signal from S1 was necessary to begin the process of event recording.

3. Counter position calibration

Using flight data, the response of the Cherenkov counter was mapped in two-dimensional space in relation to coordinates given by the MWPC system. Events possessing a rigidity greater than 2 GV, where the counter response was well above the pedestal value, were used to produce an image of the counter. The high rigidity ensured a straight trajectory in the magnetic field in the vicinity of the counters. The x and y position, where each event intersected the midplane of the counter as determined from the trajectory of the particle through the MWPC planes, was plotted and an image of the Cherenkov counter was generated.

3.1. Signal calibration

We then turned to the problem of signal calibration. The pulse heights of events as a function of R, the distance from the center of the counter to the particle's intersection with the midplane of the counter, were examined. We used only events of high rigidity (as seen by the MWPCs) that passed within the counter's boundaries as determined previously. For this purpose positive rigidity events, where 2 < Rigidity < 10 GV and negative rigidity events, where -10 < Rigidity < -0.5 GV, were employed.

For each interval of R, the most probable pulse height for the sum of all 16 PMTs was estimated as fixed percentile of the events when ranked by pulse height. The results are shown in fig. 6, where least-squares fits to a uniform distribution and a quadratic correction are shown. Since the variation is small compared to the statistical fluctuations in an individual event, which must be identified as a $\bar{p}$ or not, the uniform approximation for the sensitivity (and pathlength) is adequate.

4. Photoelectron sensitivity

To determine the average number of photoelectrons expected from a fast particle radiating the maximum Cherenkov light, we looked at the uncorrected pulse heights (no corrections for pathlength or sensitivity) from the sixteen Cherenkov PMTs with only a pedestal subtraction. We restricted our data set to a population of negative rigidity events while balloon-borne, which passed data cuts indicating a single, $Z = -1$ particle with a rigidity greater than 0.5 GV, passing through a small central region possessing 1/9 of the area of the whole Cherenkov counter.

The total number of events ($N_{total} = 518$) and the number of events that were at the pedestal (N_{zeros}) for each tube (thus, giving a zero photoelectron reading) for this subset of data were recorded. In Poisson statistics, the probability of such a zero reading is

$$P(0) = e^{-m_i} \ , \tag{2}$$

where m_i is the average number of photoelectron for the ith PMT.

Thus, an estimate $\hat{m}_i$ is given by

$$\hat{m}_i = ln(N_{total}/N_{zeros}) \tag{3}$$

for the ith PMT. Employing the above equation, we were able to estimate the expected number of photoelectrons for each of the sixteen PMTs; when these 16 numbers were added together, the total number of photoelectrons was estimated

$$n_{p.e.} = \Sigma_{i=1}^{i=16} \hat{m}_i \ , \tag{4}$$

which totaled 52.4 photoelectrons for a $\beta = 1$ particle. However, there were a few events (14) that seemed to have an anomalously low total Cherenkov output. They did not seem to be a part of the general peak. When we excluded those few events, the average total number of photoelectrons calculated from the above equation jumped to 72.2.

The expected total number $n_{p.e.}$ of photoelectrons for a singly-charged relativistic particle is

$$n_{p.e.} = \left[\left(1 - \frac{1}{n^2} \right) \frac{\Delta\omega \cdot \Delta x}{137c} \right] \epsilon_{Light\ Coll}\ \epsilon_{QE} \ , \tag{5}$$

where $n = 1.25$ is the index of refractions, $\Delta\omega = 2\pi c(1/\lambda_{min} - 1/\lambda_{max}) \cong 2.2 \times 10^{15}$ s^{-1} is the bandwidth for the R2490-01 PMT, $\Delta x = 12.1$ cm is the radiator thickness, $c = 3 \times 10^{10}$ cm/s is the speed of light, $\epsilon_{Light\ Coll} \cong 0.33$ is the light collection efficiency, and $\epsilon_{QE} \cong 0.15$ is the photocathode quantum efficiency. For the above numbers, eqs. (5) predicts $n_{p.e.} \cong 115$ photoelectrons. The wavelength shifts would increase $\Delta\omega$, but $\epsilon_{Light\ Coll}$ could be substantially lower than 0.33, if the acrylic box, waveshifter, or FC72 liquid absorbs slightly between 320 and 510 nm. When looking at the negative rigidity events, the Cherenkov peak (fig. 7) has a tail at the high intensity end. This is not evident in the analogous population of positive rigidity > 0.5 GV events (fig. 8).

The high Cherenkov tail for the negative rigidity events must be composed of showering electrons. The radiation length in FC72 is approximately 36.1 g/cm^2; the exact molecular formula of the FC fluids is a trade secret. The Cherenkov counter thickness

is 21.34 g/cm^2. Thus, more than half of the entering electrons will shower. The positive rigidity population, which is mostly protons, has little such showering activity, which explains the small tail of its distribution.

With 72.2 photoelectrons, the standard deviation is 8.5. However, due to the multiplicative ratio R_{PMT} at each PMT dynode, one expects the standard deviation at each PMT output to be increased by a factor of

$$\left(\frac{R_{PMT}}{R_{PMT}-1}\right)^{1/2} \cong 1.31 \ , \tag{6}$$

where the gains of all 16 dynodes of each PMT are assumed equal, so

$$R_{PMT} \cong (10^6)^{1/16} = 2.37 \ . \tag{7}$$

Using eqs. (7) and (6), a standard deviation of $1.31(72.2)^{1/2} = 11$ photoelectrons would be expected. Figure 9 shows the distribution of total pulse height observed in a set of high rigidity positive and negative muons at ground level; its width is a factor of 1.38 larger than predicted on the basis of eqs. (2)-(7), corresponding to a standard deviation of 15 photoelectrons. Thus, the level of maximum Cherenkov light and 50% of that level are separated by 2.4 standard deviations.

Figure 10 shows an "isovariant" distribution for positive particles at 5g/cm^2 atmospheric depth of Cherenkov response vs. magnetic deflection constructed by plotting $k(I_c)^{1/2}$ vs. $\mathcal{R}^{-1}$, the inverse rigidity; these variables have approximately constant, Gaussian-distributed errors independent of their magnitudes, and the constant k has been adjusted so that the errors in the vertical and horizontal (and any direction) are the same. The points for particles of a given mass are expected to fall on an ellipse, which, by accident, is a circle for the protons. The points extending to the right of the circle are due to the Cherenkov light emitted by the acrylic box. The ellipse of points with a doubled vertical major axis and a halved horizontal minor axis is due to alpha particles.

Figure 11 is similar to Fig. 10, but for negative particles with $(I_c/I_{c,max})^{1/2}$ on the vertical axis and $1.15/\mathcal{R}$ on the horizontal axis. Sectors 1 and 2, as well as $(I_c/I_{c,max})^{1/2} >$

0.72 have been cut from the data. The circular areas show the $\pm 1\sigma$ region for antiprotons. Three antiproton candidate events can be seen in the $\pm 1\sigma$ region below $(I_c/I_{c,max})^{1/2} < 0.6$. The point just inside the inner circle is consistent with the number of antiprotons which would be expected to lie outside $\pm 1\sigma$. (The horizontal line of points with $(I_c/I_{c,max})^{1/2} \approx 0.72$ is the tail of a distribution centered at $(I_c/I_{c,max})^{1/2} = 1$ due to negative electrons, muons, and pions.)

5. Conclusion

It was disappointing that, although the Hamamatsu R2490-01 PMT did give high gain in a magnetic field, its pulse-height resolution was poor. Using our 662 keV ^{137}Cs light source, direct comparisons with the RCA8575 PMT indicated that the Hamamatsu R2490-01 had a line width that was a factor of 2 wider. An improved PMT for use in magnetic fields is needed.

The FC72 liquid containment and filling system performed perfectly, with little or no loss of liquid due to the flight and recovery. Although lab tests during the design of the counter indicated that the waveshifter fluors were insoluble in FC72, it was found after the flight that some had dissolved into the liquid. This indicates that coating the inside walls of the acrylic box with waveshifts might be unnecessary. The background Cherenkov radiation from the top and bottom acrylic wall might be eliminated or reduced by either (a) developing a high-efficiency white coating which remains unaffected by contact with FC72 or (b) protecting the white coating with acrylic or Mylar sheets thinner than the 4.8 mm acrylic employed by us, yet thick enough to maintain a sealed enclosure for the FC72.

We gratefully acknowledge the assistance during the design, testing, and assembly of the Cherenkov counter at the University of Arizona by Professor D. R. Huffman for the use of optical equipment, by Peter Halverson for the design of the pulse amplifier, and by M. Damento and S. Syracuse for assembly and testing.

References

[1] R.L. Golden, G.D. Badhwar, J.L. Lacy and J.E. Zipse, Nucl. Instr. Meth. 148 (1978) 179; R.L. Golden et al., Phys. Rev. Lett. 43 (1979) 1196.

[2] R.E. Streitmatter et al., Advan. Spa. Res. 9 (1989) 1265.

[3] J.V. Jelly, Cherenkov Radiation and its Applications (Pergamon Press, UK, 1958) pp. 1-31.

[4] 3M Product Manual: Fluorinert Electronic Liquids, Commercial Chemical Division/3M (1985).

[5] W. Viehman and R.L. Frost, Nucl. Instr. Meth. 167 (1979) 405.

[6] T. Bowen, D.A. DeLise and A.E. Pifer, Phys. Rev. C 14 (1976) 195.

[7] F. Grum and G.W. Luckey, App. Opts. 7 (1968) 2289; C.M. Shai and J.B. Schutt, Goddard Space Flight Center Print X-762-71-266 (1971).

[8] J.D. Jackson, Classical Electrodynamics, 2nd Ed. (John Wiley and Sons, NY, 1975) pp. 638-641.

[9] The polyethylene reservoir was a standard automobile radiator overflow reservoir.

[10] Particle Data Group, Phys. Rev. Lett. 170B (1986).

[11] R.L. Golden, LEAP Configuration Guide, Particle Astrophysics Laboratory, New Mexico State University, Las Cruces, NM (1987).

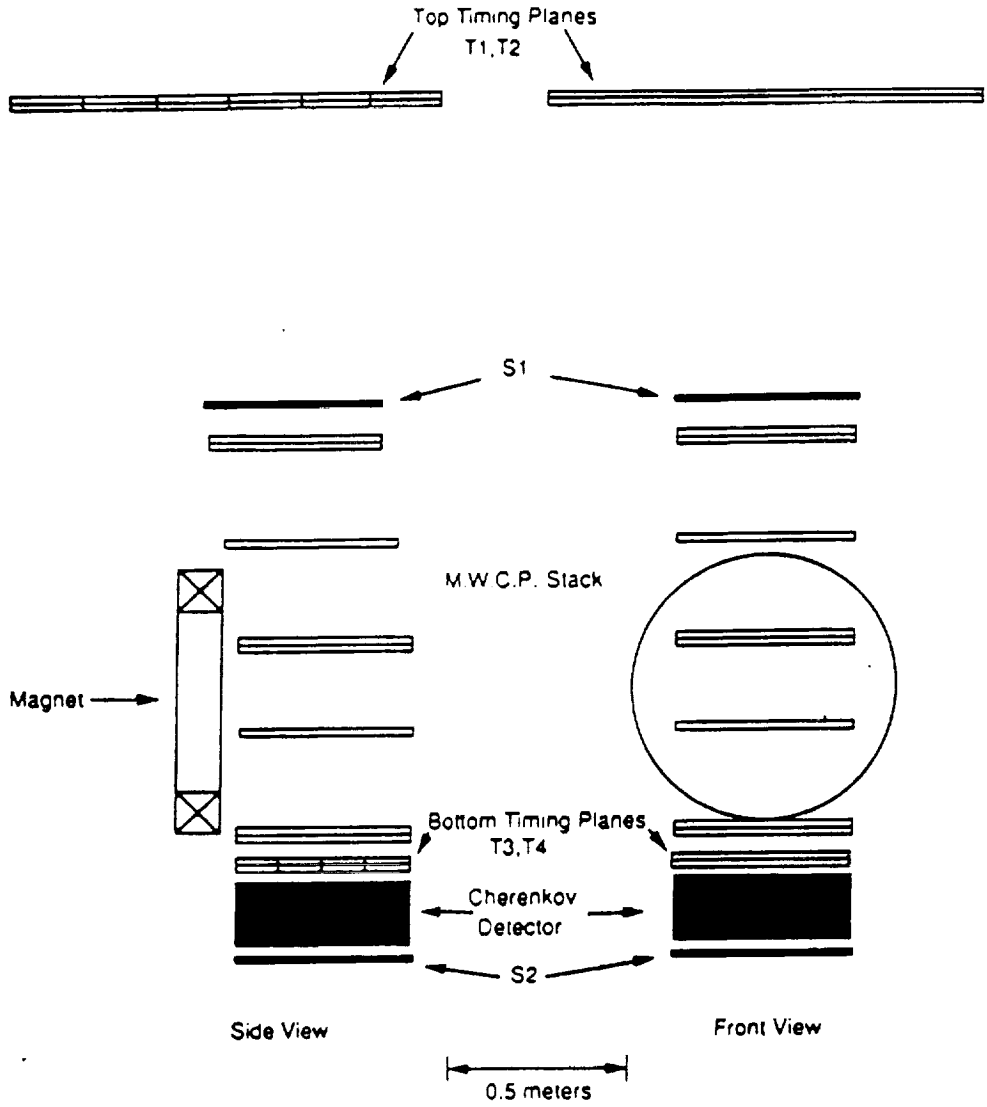

Fig. 1. The LEAP experiment, consisting of T1, T2, T3, T4 (the time-of-flight detector); S1, S2 (scintillation detectors); MWPC stack and magnet (the NMSU magnet spectrometer); and the Cherenkov detector.

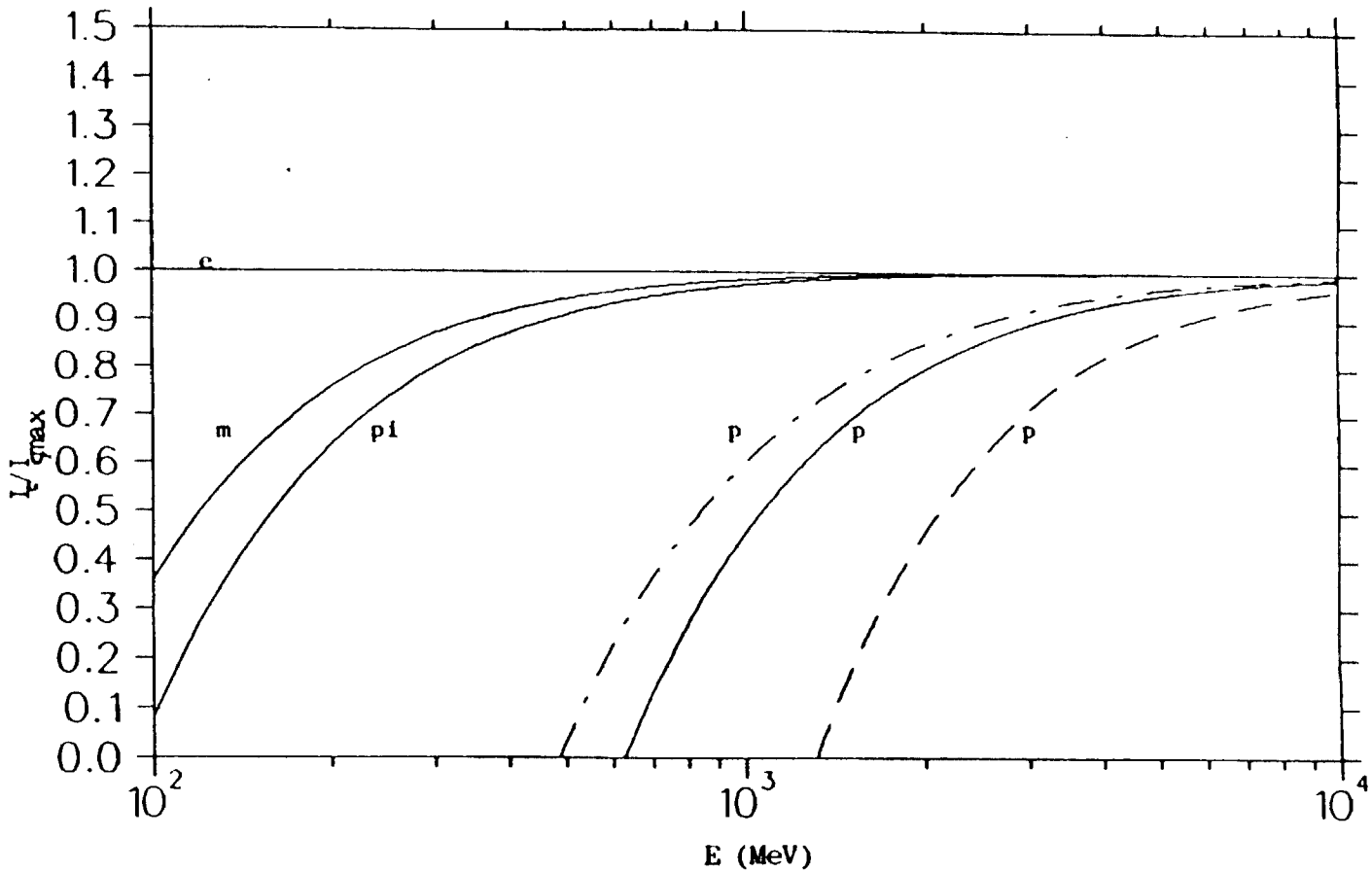

Fig. 2. The Cherenkov light L/L_{cmax}, where L_{cmax} is the maximum Cherenkov light for a Z=1 particle, as a function of kinetic energy E. The solid curves are for n(ref)=1.25. The dashed curve is for n(ref)=1.1. The dot-dashed curve is for n(ref)=1.33. Particles shown are: e, electrons; p, protons and antiprotons; m, muons; pi, pions.

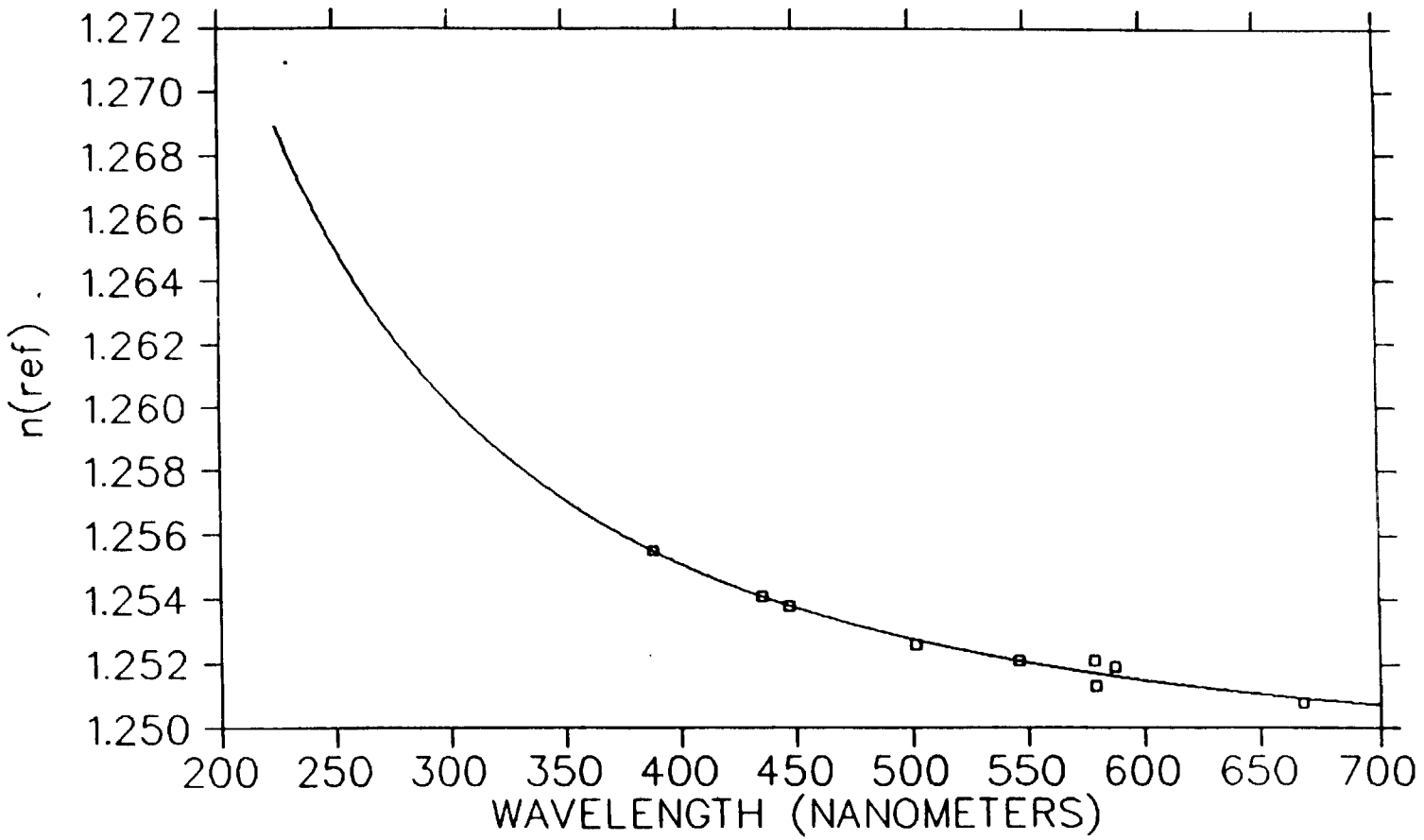

Fig. 3 The index of refraction as a function of wavelength of FC72 at 24.0°C +/- 0.2°C. The experimental data is shown as boxes.

The fitted curve is a form of Cauchy's equation

n(L) = A + B/L**2 + C/L**4

where L is wavelength and A, B, and C are fitted parameters.

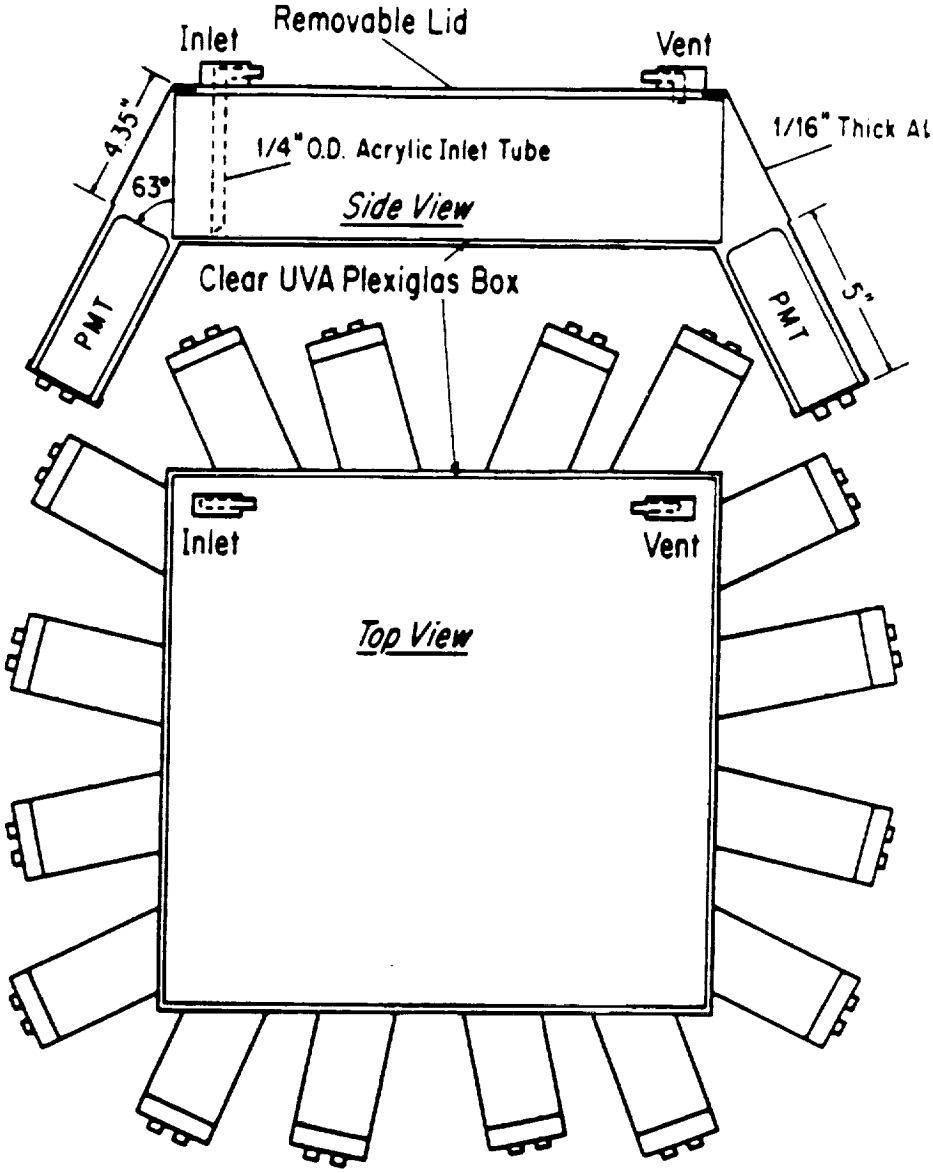

Fig. 4 Side and plan views of the Cherenkov detector, showing the aluminum box surrounding a clear UVA plexiglas box, which is coated on the inside with wavelength shifter dyes, and which contains the FC72. The 16 Hamamatsu R2490-01 PMT's view the FC72 along the four sides (four PMT's to a side).

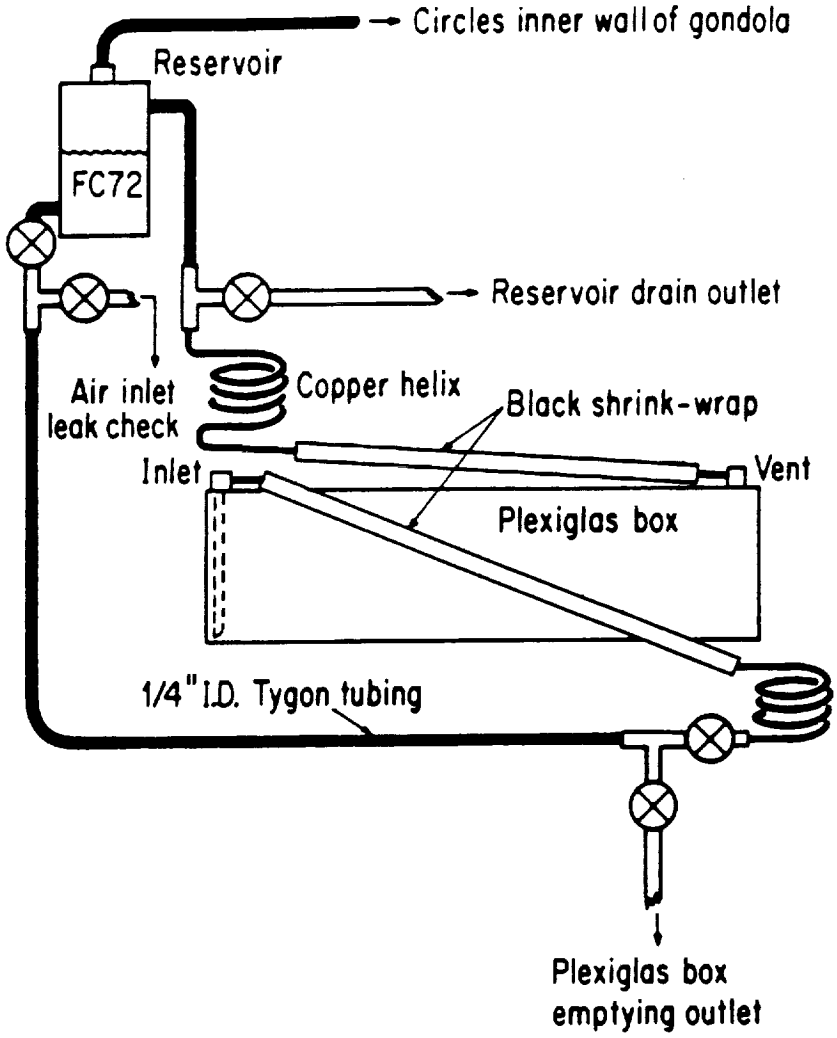

Fig. 5 . The FC72 filling system, with 2 liter capacity reservoir. The plexiglas box shown rests within the aluminum box.

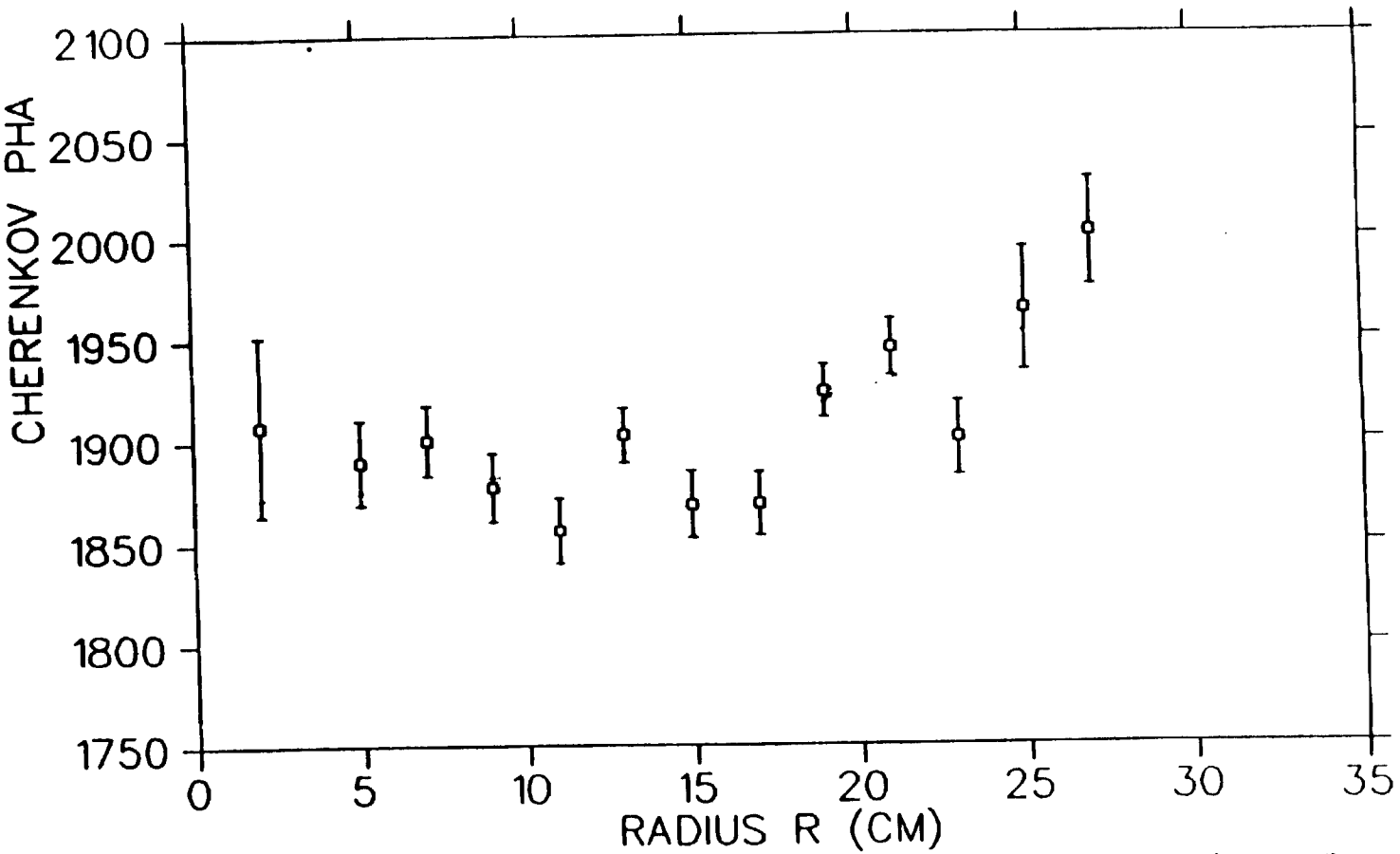

Fig. 6 The pulse height peak positions as a function of the radius from the center of the Cherenkov counter for high rigidity events.

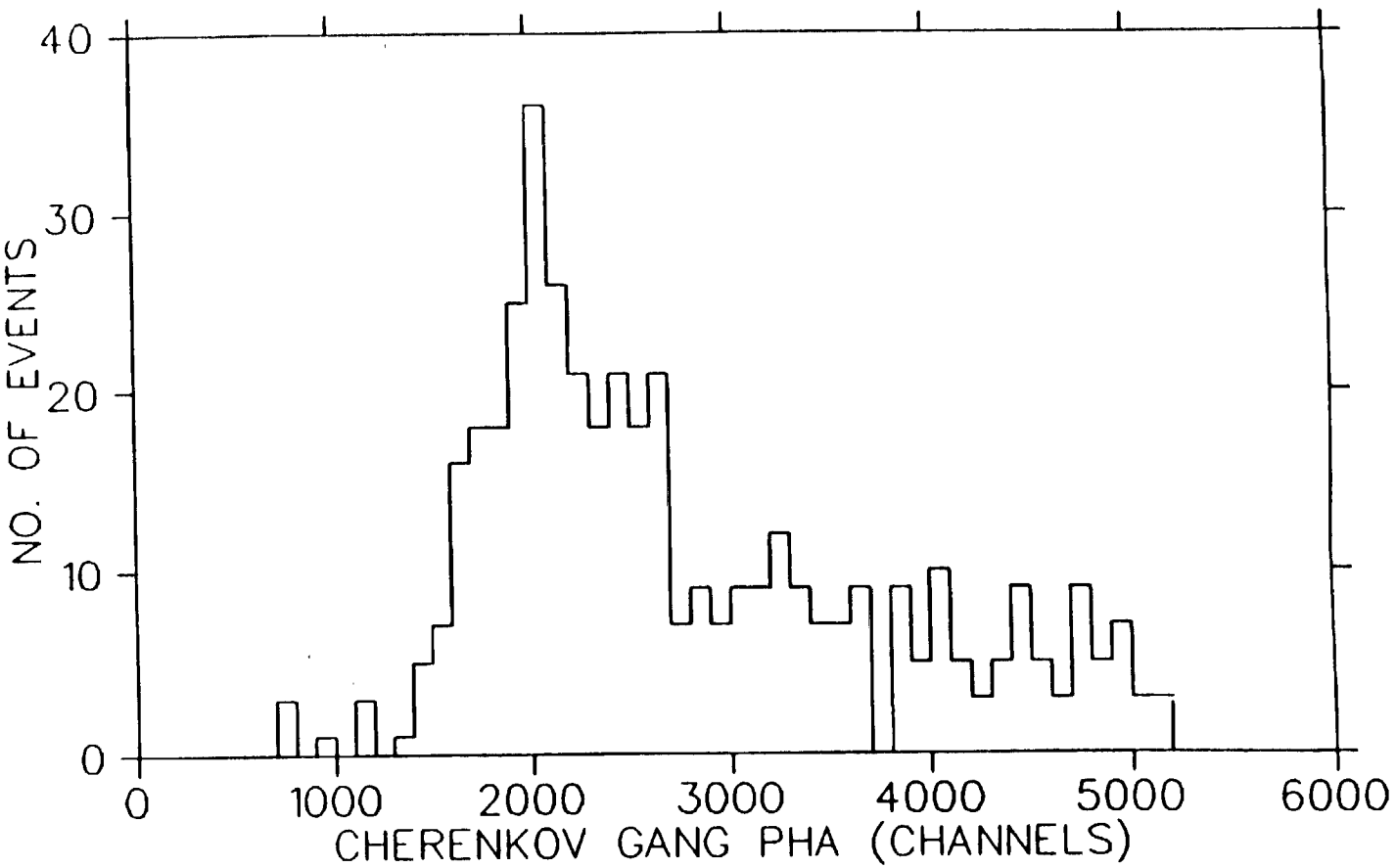

Fig. 7 The Cherenkov gang PHA from the central region of the counter for negative rigidities greater than 0.5 GV.

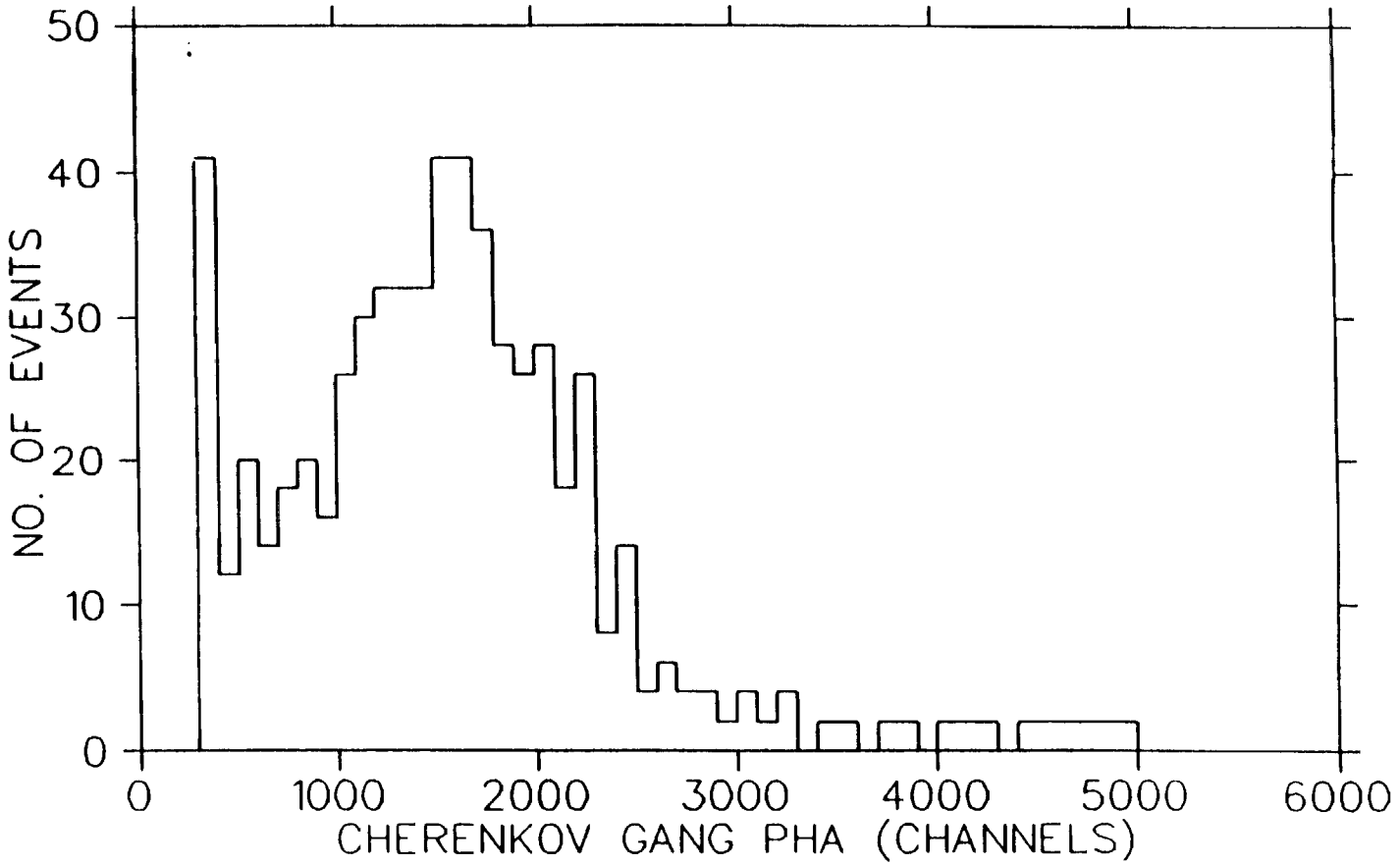

Fig. 8 The Cherenkov gang PHA from the central region of the counter for positive rigidities greater than 0.5 GV.

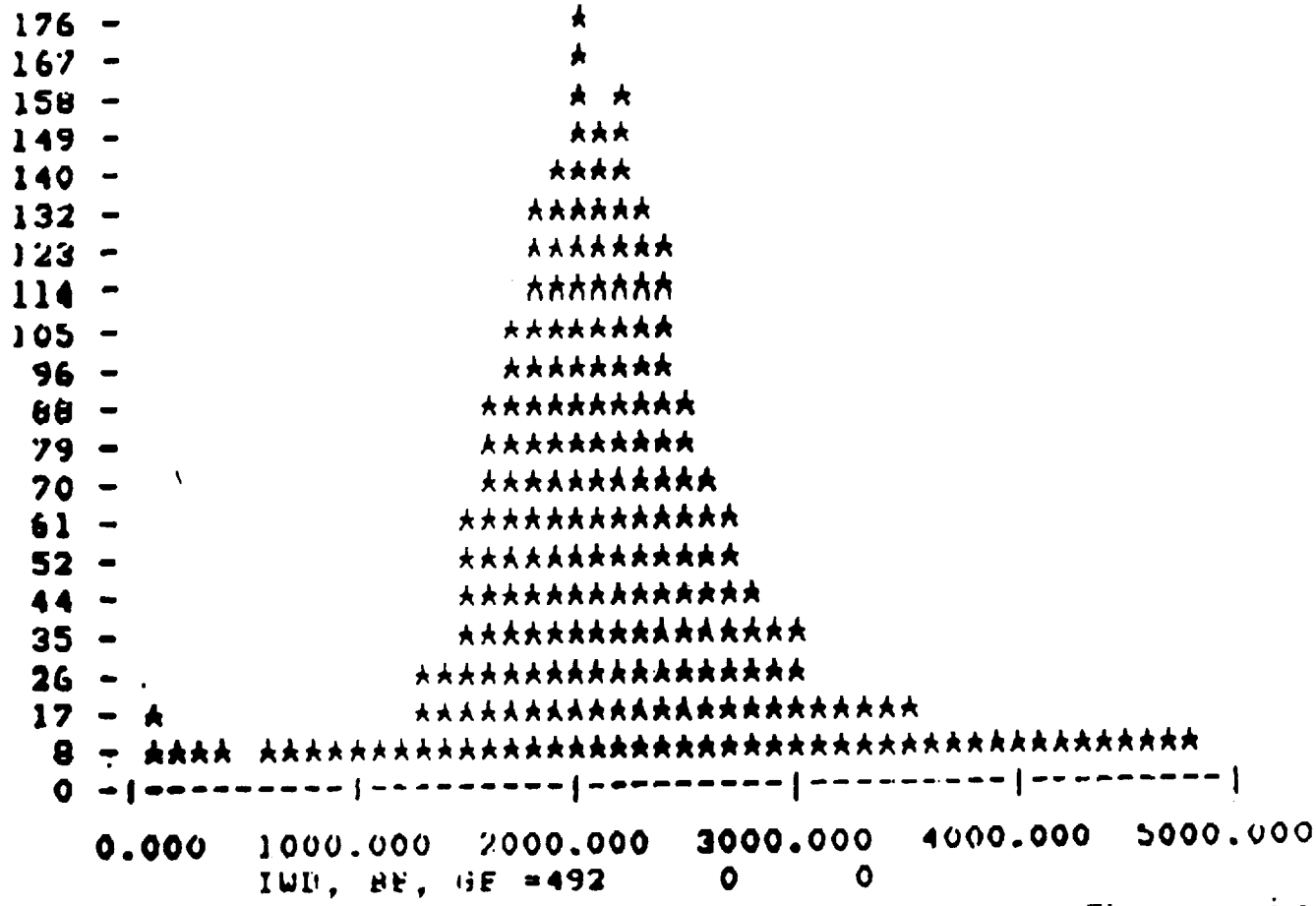

Fig. 9 A histogram of high rigidity events. The x axis the sum of the pulse-heights of all 16 PMT's.

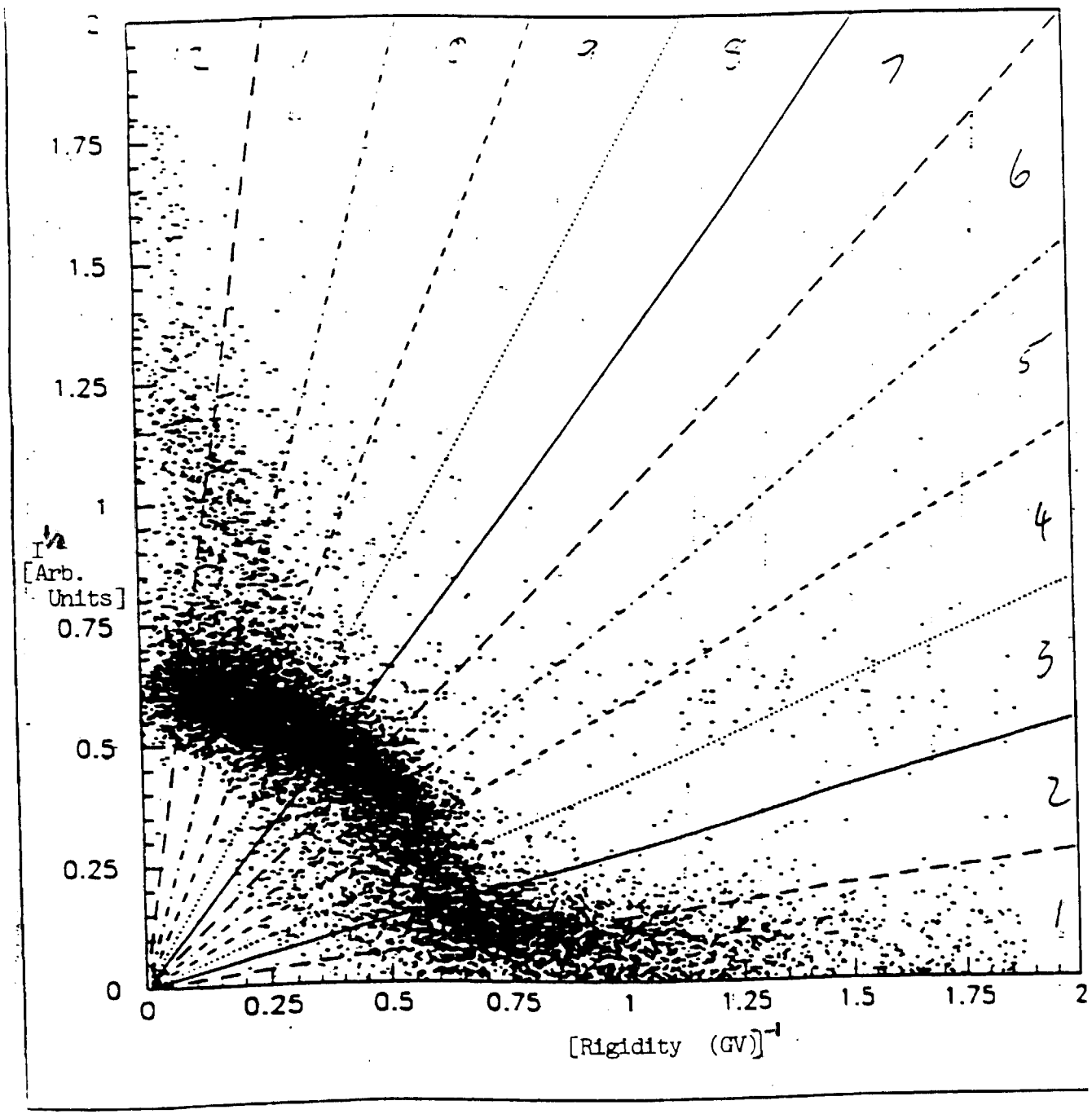

Fig. 10 The square root of the Cherenkov signal vs. inverse rigidity, with the vertical axis adjusted for equal errors vertically and horizontally. The quadrant of a circle is due to protons radiating in FC-72. The points with $(\text{Rigidity})^{-1} > 0.7$ are due to protons radiating in the acrylic top and bottom of the FC-72 container. A fainter ellipse of α-particle points is also visible with a vertical major axis = 1.25 units and a horizontal minor axis = 0.3 (GV)-1.

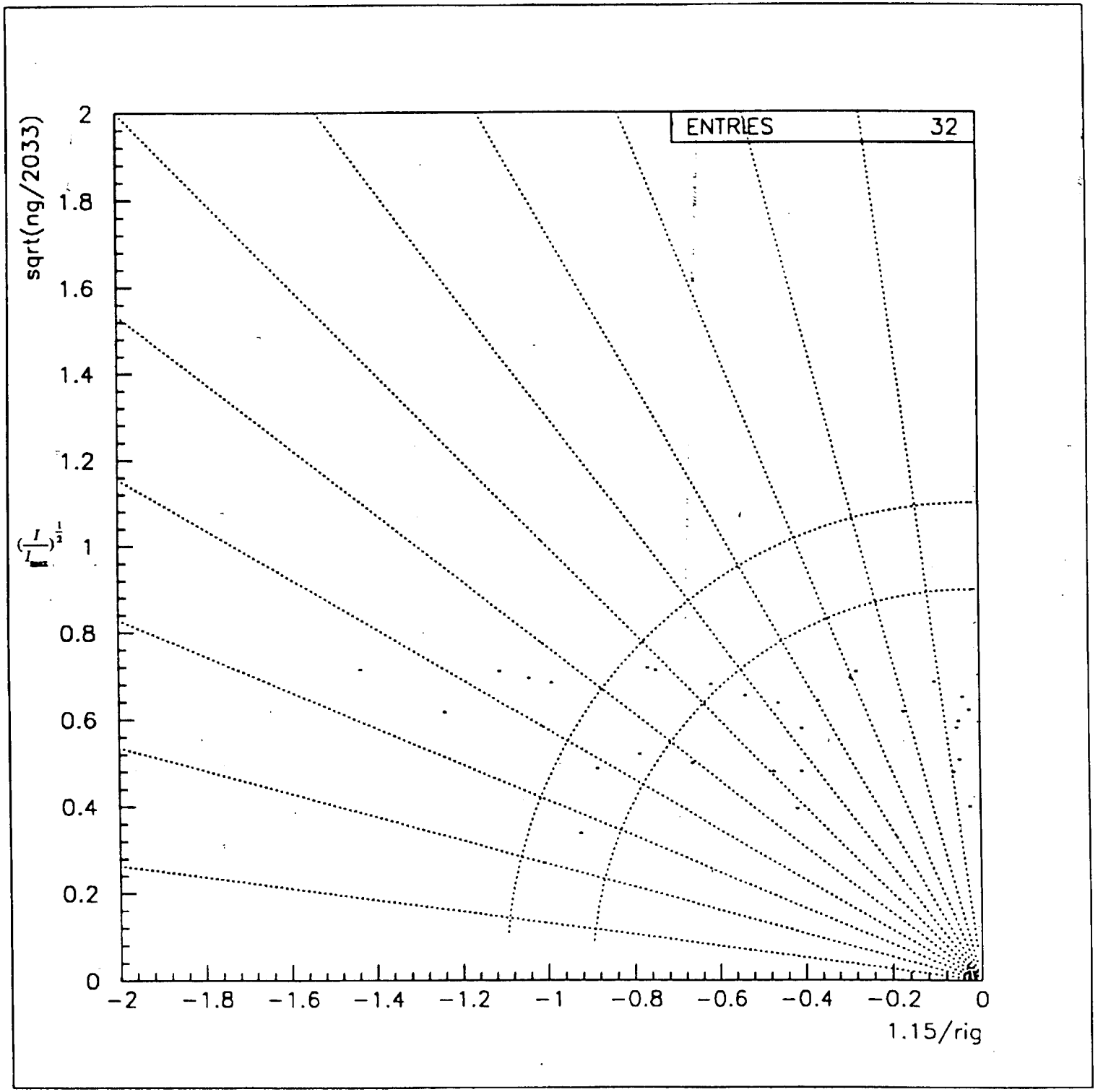

Fig. 11. This "isovariant" plot shows $(I/I_{max})^{½}$ vs. 1.15/rigidity for each event, with equal statistical errors in anydirection, for all negative rigidity events with $(I/I_{max})^{½}<0.7$ as described in the text. The circles indicate the $\pm 1\sigma$ region for antiproton canidates.